A field study (Massachusetts, USA) of the factors controlling the depth of groundwater flow systems in crystalline fractured-rock terrain

David F. Boutt · Patrick Diggins · Stephen Mabee

Abstract Groundwater movement and availability in crystalline and metamorphosed rocks is dominated by the secondary porosity generated through fracturing. The distributions of fractures and fracture zones determine permeable pathways and the productivity of these rocks. Controls on how these distributions vary with depth in the shallow subsurface (<300m) and their resulting influence on groundwater flow is not well understood. The results of a subsurface study in the Nashoba and Avalon terranes of eastern Massachusetts (USA), which is a region experiencing expanded use of the fractured bedrock as a potable-supply aquifer, are presented. The study logged the distribution of fractures in 17 boreholes, identified flowing fractures, and hydraulically characterized the rock mass intersecting the boreholes. Of all fractures encountered, 2.5% are hydraulically active. Boreholes show decreasing fracture frequency up to 300m depth, with hydraulically active fractures showing a similar trend; this restricts topographically driven flow. Borehole temperature profiles corroborate this, with minimal hydrologically altered flow observed in the profiles below 100m. Results from this study suggest that active flow systems in these geologic settings are shallow and that fracture permeability outside of the influence of large-scale structures will follow a decreasing trend with depth.

D. F. Boutt (✉) · P. Diggins
Department of Geosciences,
University of Massachusetts-Amherst,
611 N. Pleasant St., 233 Morrill Science Center,
Amherst, MA 01002, USA
e-mail: dboutt@geo.umass.edu
Tel.: +1-413-5452724
Fax: +1-413-5451200

P. Diggins
Environmental Resources Management (ERM),
399 Boylston St., Boston, MA 02116, USA

S. Mabee
Office of the State Geologist,
University of Massachusetts-Amherst,
611 N. Pleasant St., 233 Morrill Science Center,
Amherst, MA 01002, USA

Introduction

Fractured igneous and metamorphic rocks, characterized by low matrix permeability and strongly preferential flow paths, are increasingly being used as a primary source of potable water throughout the world, as places to store various types of waste (i.e. spent nuclear fuels), and as geothermal reservoirs. These rocks generally have very low porosity (<1%) and, hence, have limited ability to store water. The hydrogeologic properties of fractured crystalline rocks are determined by the existence, aperture, and connectivity of discrete features (i.e. fractures and faults). The hydrogeologic setting (saturation state, hydraulic gradient, etc.) of these rocks controls the occurrence, nature, and rate of fluid movement. Fracture permeability in crystalline rocks varies over several orders of magnitude, exhibits considerable spatial variability over short distances, and can demonstrate a sharp decrease with depth (NRC 1996). Hydrogeologists have documented that water wells in crystalline rock, in general, and in rocks of Pre-Cambrian age in particular, have low yields (Meinzer 1923). Early data on yield of water wells in crystalline rocks commonly suggested that the network of open joints is principally maintained within 100–150 m of the land surface (Davis and Turk 1964; Legrand 1954; Legrand 1967). It has been suggested and theorized that the abundance and aperture of fractures decrease with depth, and these changes contribute to downward decrease in porosity and permeability (Snow 1968; Ruqvist and Stephansson 2003; Maréchal et al. 2004). Little quantitative data exists on the nature of these trends and how the depth evolution of different fracture sets contributes to the bulk hydraulic properties of these rocks (Mazurek 2000). The purpose of this report is to define and clarify the extent of this generalization and the factors that control the potential depth evolution of hydraulic properties at a regional scale by collecting high-quality borehole geophysical data in boreholes at various distances from major structural features.

A watershed-scale US Geological Survey (USGS) research program at Mirror Lake, New Hampshire (USA), studying multi-scale properties and characterization of

groundwater flow and chemical transport in fractured rock (Shapiro et al. 2007), has yielded tremendous insight into crystalline fractured rock environments. Local-scale investigations have been conducted over distances of tens of meters and focused on identification of fractures and fracture properties in outcrops (Barton 1996), fractures in the subsurface using borehole and surface geophysics (Johnson and Dunstan 1998; Paillet 1985; Paillet and Kapucu 1989), and hydraulic and transport properties of fractures by means of hydrologic testing (Hsieh 1996; Hsieh and Shapiro 1996; Tiedeman and Hsieh 2001). Results presented by Shapiro and Hsieh (1998) on the transmissivity distribution in boreholes ranging from 20 to 170 m depth indicate that the most transmissive fractures zones were found in the upper 50 m of the borehole and showed a decrease with depth. Examination of well-bore derived fracture distributions suggests that the density of hydraulically substantial fractures in crystalline aquifers is low in relation to the total fracture density (e.g., Snow 1968; Shapiro and Hsieh 1991; Shapiro and Hsieh 1994; Mazurek et al. 2003). The pattern of few hydraulically substantial fractures is also present along drifts at the Äspö Hard Rock Laboratory in Sweden, where more than 100 free-flowing, steeply dipping, decameter-scale fractures are observed with a spacing (average distance between two fractures) of 10–20 m with individual transmissivity values above 10^{-6} m^2/s, rendering a hydraulic fracture density of 0.05–0.10 fractures per meter (Mazurek et al. 2003). Evans et al. (2005) demonstrated that at deeper crustal levels only 20% of the fractures detected in the Soultz-sous-Forets (France) Hot Dry Rock site's granite wells are hydraulically active.

Although fractures in crystalline rocks appear to be strongly heterogeneous, attempts are being made to characterize brittle structures and their controls on regional flow systems. Delineation of packages of rocks, based on some physical attribute, offers a way of characterizing aquifers at a regional scale where fracture distributions and properties are more heterogeneous than at the local scale. For example, Caine and Tomusiak (2003) utilized field-based geologic and fracture characterization techniques to establish geologic controls on subsurface hydraulic properties of fractured crystalline rocks. The applied techniques were used to delineate potentially significant hydrogeologic units in the ~120 km^2 Turkey Creek watershed in the state of Colorado (USA). The hydraulic properties of the units were based primarily on the nature and distribution of fractures that were observed in outcrop. Numerical simulations of groundwater flow in synthetic discrete fracture networks provided upper bound estimates of aquifer properties of each unit that was delineated. Estimates from each model representing particular units were also used to evaluate the relative hydraulic properties between outcrops and to assess the geologic controls on storage and regional flow. Rock type alone is commonly of secondary importance and these statements are quantitatively supported by the work of Caine and Tomusiak (2003) and Surrette and Allen (2008).

Another way of delineating hydrogeologic units is based on hydrostructural domains, which are units of rocks with similar fracture intensities and, thus, potentially similar transmissive and storage properties (Mackie 2002). Working in folded and faulted sedimentary rocks of the Gulf Islands, British Columbia (Canada), Surrette et al. (2007) quantified regional-scale relative potential transmissivity and permeability patterns using the hydrostructural domain approach; they found that transmissivity increased towards the southeast along the island chain. A three-dimensional model and approach was developed to estimate the transit time for a groundwater flow system in fractured bedrock of the Canadian Shield (Park et al. 2008). A decreasing trend with depth of permeability structure of the fractured bedrock was observed but it was not consistently observed across all of the structures in the study area. Uncertainty in how the permeability structure is modified with depth was the most significant factor determining the transit time in this crystalline rock environment. Regional-scale tectonic structures such as fault zones, have been acknowledged and attributed to the permeability structure at depth within the shallow (Seaton and Burbey 2005) and the deep (Stober and Bucher 2004) crusts. Faults modify the regions in their vicinity by acting as conduits or barriers to flow (Caine et al. 1996). These studies have, for the most part, ignored how the physical and hydrologic characteristics of fractured crystalline rock aquifers evolve with depth at a regional scale.

In this report, the results of a regional-scale integrated study of the physical and hydrogeologic properties of a fractured crystalline rock unit in eastern Massachusetts (USA), using borehole geophysical logging and single well hydraulic tests, is presented. This study avoids the direct use of driller data (such as yield, encountered fracture statistics, and water-bearing fracture statistics) but relies on high-quality geophysically derived borehole data to answer important questions regarding the depth-dependent physical and hydraulic properties of fractures in the shallow subsurface. Seventeen uncased fracture rock boreholes were studied, compiling fracture types, orientation, and hydrologic characteristics for wells at various distances from regional structural features. This report describes the geology of the region, including the results of previous surface-based fracture mapping, followed by a detailed analysis of the borehole geophysical logs, and concludes with implications of the hydrogeological data for the management of this important aquifer system. The significant contribution presented here is the integrated data-collection efforts at a large scale with an emphasis on the tectono–structural assemblages that give rise to observed depth-dependent characteristics of the rock mass for shallow hydrologic-flow systems.

Fractured igneous and metamorphic rocks of eastern Massachusetts

The rocks investigated in this study consist of fractured crystalline igneous and metamorphic rocks of the Nashoba

and Avalon terranes of eastern Massachusetts. They range from massive, non-foliated intrusives to high-grade foliated metamorphics and are representative of many crystalline bedrock aquifers throughout the world. Massachusetts geology is the amalgamation of rocks from three tectonic plates. These rocks include those associated with the margin of the Laurentia plate, the medial New England plate (which includes Ordovician-age intrusive and extrusive rocks associated with an island-arc system and Proterozoic rocks of uncertain origin) and the Avalon plate. These plates were active during the early to middle Paleozoic (Robinson et al. 1993). Structural and metamorphic features were produced during three orogenic events. These include the late Ordovician Taconian Orogeny (the docking of medial New England with Laurentia, affecting central and western Massachusetts), the Devonian Acadian Orogeny (the docking of Avalon with amalgamated Laurentia and medial New England, affecting eastern and central Massachusetts predominantly) and the Pennsylvanian-Permian Alleghenian Orogeny (metamorphism and reactivation of faults produced by the collision of Africa with North America). All structures were later modified and potentially reactivated by extension in the Mesozoic during opening of the present day Atlantic Ocean (Robinson et al. 1993). The Bloody Bluff fault zone is the main suture zone connecting the Avalon Terrane with the rest of New England (Fig. 1). These features are mapped as major ductile shear zones that have varying degrees of brittle-tectonic features. The Avalon Terrane extends from the Bloody Bluff fault zone southeastward into the Atlantic Ocean (Hatch 1991). The Avalon Terrane primarily contains a variety of foliated and non-foliated granites with some gneisses, quartzites and metavolcanics. Sandwiched between medial New England and Avalon is an enigmatic terrane referred to as the Nashoba Terrane (Fig. 1). The Nashoba Terrane was not accepted as a separate terrane until the early 1980s following identification of the large terrane-bounding ductile shear (fault) zones (Castle et al. 1976; Bell and Alvord 1976). The Clinton Newbury fault zone delineates the western edge of the Nashoba Terrane and separates it from the eastern portion of medial New England, an area known as the Merrimack Belt (the Merrimack Belt lies within the Merrimack Synclinorium and forms the eastern half of medial New England) (Fig. 1). Rocks of the Merrimack Belt are comprised of calcareous metasiltstones, phyllite, metasandstones and quartzites of Silurian and Ordovician age (Robinson and Goldsmith 1991). The rocks immediately west of the Clinton-Newbury fault are metamorphosed to the lower greenschist facies and
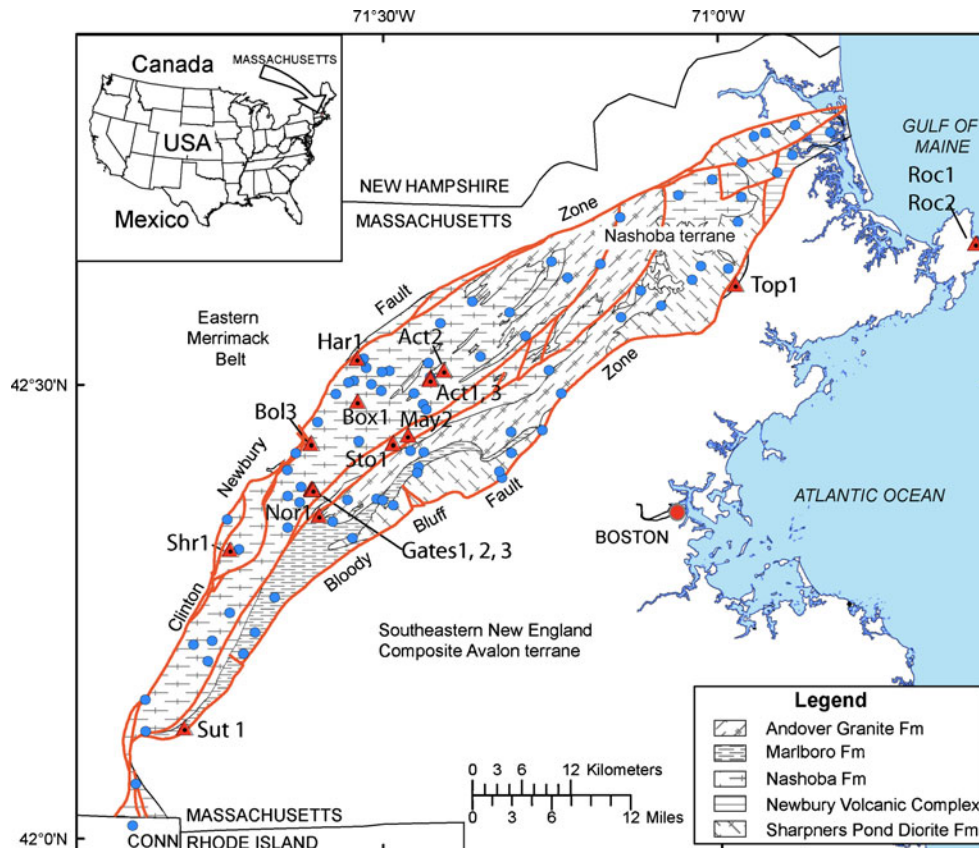
Fig. 1 Map of eastern Massachusetts showing the geographic distribution of the lithotectonic packages of the *Eastern Merrimack Belt*, *Nashoba Terrane* and Avalon Terrane. Outcrops described by Manda et al. (2008) are shown as *blue circles*, whereas wells where borehole geophysical measurements were conducted are shown as *red triangles*. Terrane bounding and major inter-terrane faults are shown as *red lines*

progressively rise in grade toward the northwest. The rocks of the Nashoba Terrane, east of the Clinton-Newbury fault, are multiply deformed and metamorphosed middle to upper amphibolite facies rocks (sillimanite and silli-manite-K feldspar zones) consisting of largely meta-volcanic materials to the east and metasedimentary rocks to the west (Goldsmith 1991). Small ductile shear zones separate these distinct units (red lines in Fig. 1). Of the boreholes studied in this project, 15 are in the Nashoba Terrane with only 2 in the Avalon Terrane (Fig. 1).

Results from previous outcrop and roadcut investigations

Over the last 6 years, fracture characterization data has been collected by the authors as part of geologic mapping efforts in the Avalon and Nashoba terranes. To date, 10 new 1:24,000-scale bedrock geologic maps with associated fracture characterization data have been prepared (e.g., Mabee and Salamoff 2006). This represents over 12,000 brittle fracture measurements collected from more than 500 outcrops. Data from over 3,000 wells have also been assembled in a geographic information system (GIS) format in the same quadrangles for which fracture data have been collected, allowing preparation of depth to bedrock, bedrock water table and yield distribution maps, among others.

Based on this previous work and the work of Manda et al. (2008), several general observations can be made about the character of the fractured rock environment. Manda et al. (2008) identified three main types of fractures present in these rocks: foliation parallel fractures, tectonic joints, and sheeting (subhorizontal unloading) joints. These three fracture types represent three conditions observed in the field that have demonstrated control on flow anisotropy and permeability characteristics. For example, in West Newbury, Massachusetts, two public water supply wells located in phyllite that exhibited foliation parallel fractures (FPFs) formed an elongated cone of depression parallel to the foliation (Lyford et al. 2003). Sheeting joints can dominate the flow field in the upper 15 m of the crust but do not develop equally in all rocks depending on lithology or the presence or absence of foliation. In contrast, FPFs develop along penetrative fabric and can exhibit open fractures with depth. In places where the dominant foliation is shallow, shallow dipping FPFs dominate the flow regime instead of sheeting joints. As an example, flow to two wells drilled to depths of 152 m in Paxton, Massachusetts, received most of their water from partings parallel to foliation that dipped 10° to the east (Lyford et al. 2003). In regions where sheeting joints are present, they play the largest role in conducting fluids in the shallow subsurface, whereas tectonic and steeply dipping FPFs act as the major vertical connecting joints.

Other general observations are included in the following. Firstly, foliation and foliation parallel fractures (FPFs) are sub-parallel to the axis of the Nashoba Terrane: foliation trends are north northeast in the south and gradually rotate to northeast in the north (Fig. 1). The foliation is a penetrative fabric observed in tunnels and borings that exceed depths of 200 m. However, locally within some of the granites, the foliation is variable. Secondly, FPFs are common in the metamorphic rocks and granitic gneisses. They are best developed in amphibolites, foliated granitic gneisses and altered and sheared rocks associated with fault zones. Thirdly, the dominant regional tectonic joints are steeply dipping northwest- and northeast-trending fractures; and fourthly, although the median trace lengths of FPFs are comparable to joints, the spacing for FPFs is half that of steep joints. The fifth observation is that trace length and spacing distributions of FPFs are controlled by lithology and the degree of development of foliation and the sixth is that massive granites exhibit a regional north–south and east–west fracture pattern, often known as 'rift and grain' by quarry operators. The rift and grain is controlled by closely spaced microscopic fracture planes in quartz that are now healed into thin zones of very tiny fluid inclusions (Wise 2005). Seventhly, subhorizontal sheeting joints are prevalent at the surface and decrease in frequency with depth. Sheeting joints are most common in rocks that are massive or in rocks that are foliated with dips >50°. Sheeting in the massive rocks also tends to have longer trace lengths. Eighthly, sheeting does not tend to develop in foliated rocks with dips less than 50°. Here, fractures form parallel to the existing foliation as confining stress is released. Any sheeting that does develop terminates against compositional foliation and has very short trace lengths (<1 m). The ninth observation is that fracture zones, or discrete zones of closely spaced fractures, are most common in the massive granites and portend a nearby fault (the frequency of fracture zones tends to increase proximal to brittle faults), while the tenth is that foliated granites provide the most consistent, orthogonal networks of interconnected fractures. Despite the details provided by these investigations current understanding of how these trends translate into subsurface remains obscured. Thus, hydrogeologists now focus on the newly acquired subsurface data using downhole measurements.

Methods

Structural and hydrogeologic settings of studied wells

During the summer of 2007, a project was undertaken to log previously drilled wells within the Nashoba and Avalon terranes using a suite of borehole geophysical tools. This study was undertaken to determine the number, type, and characteristics of fractures in various rock types that participate in flow and to compare the fracture characterization to data collected from outcrops with data derived at depth in the borehole. Wells chosen for detailed logging and characterization were chosen based on availability of the well, and permission to access it, which was primarily a function of the well not having downhole instrumentation or pumps. All wells used in this study were drilled for either individual or public water supply

purposes and not for scientific reasons. Therefore the ages of the wells were not all the same and varied from as young as 6 months to 15 years (Table 1).

As described in the previous, the Nashoba and Avalon terranes are composed of heavily deformed igneous and metamorphic rocks separated by highly deformed ductile shear zones. Ten of the 17 wells (Act1, Act2, Act3, Bol3, Box1, Gates1, Gates2, Gates3, Har1, and Nor1) logged during this study are located in the Nashoba Formation, a fine-to-medium grained, well foliated, gray-to-silvery-gray quartz-mica schist that may contain biotite, garnet and sillimanite. Four wells (May2, Shr1, Sto1, and Sut1) are located in an unnamed amphibolite-gneiss unit. It is primarily a fine-to-medium grained hornblende-actinolite-biotite-quartz-plagioclase orthogneiss with strongly defined lineation. These units lie between the schist of the Nashoba Formation and large mapped ductile shear zones in the Nashoba Terrane. Two wells (Roc1 and Roc2) lie outside the Nashoba Terrane (Avalon Terrane) in the Cape Ann Granite. The Cape Ann granite is a medium-to-coarse-grained leucocratic rock. The composition in the area of the wells is alkali-feldspar syenite. A single well (Top1) lies in a medium-to-fine-grained light-pink granodiorite that intrudes gneiss adjacent to the Bloody Bluff Fault zone. Of the number of mapped ductile faults, both terrane bounding and interior, all wells studied (with the exception of Roc1 and Roc2) lie within 4 km of a fault (Table 1) and the majority lie with 1 km of faults. Roc1 and Roc2 are both located within 500 m of a north northeast trending brittle fault in the Cape Ann Granite (not shown in Fig. 1 due to scale). Approximate distances are listed in Table 1.

The hydrogeologic setting of individual borehole sites varied significantly; sites are located in large river valleys, on hill tops, and on the coast. Borehole elevation above sea level ranged from 178 to 131 m. The depth to water averaged 8 m below land surface (Fig. 2). The maximum depth to water was 23 m below the land surface and there was one flowing well. Roughly half of the wells are interpreted to be weakly-to-semi-confined having hydraulic heads reaching into the casing above the bedrock interface. Most of the wells plot on or near a 1 to 1 line of hydraulic head versus land surface elevation, indicating a topographically driven flow system that is not strongly confined (Fig. 2). The measurement of head above the land surface is not easily made and does not preclude this data, indicating weakly confined conditions; however, only one well (Nor1) in this study exhibited weak flowing conditions.

Borehole geophysical logging

In a geologic setting dominated by highly metamorphosed igneous and fractured rock, such as the Nashoba and Avalon terranes, borehole geophysical tools are useful in conjunction with surface mapping for the following reasons: to determine a detailed profile of the borehole fluids and the rock units, to identify and measure discrete fractures or fracture zones in the rock, and to identify which discrete fractures are contributing to groundwater flow and at what magnitude. The data collected by these tools provide a detailed picture of the subsurface that could not be obtained otherwise. Proper and effective use of these tools has been laid out by several authors in the past, so methods described here follow those studies (Johnson and Williams 2003).

A suite of five tools, designed by Advanced Logic Technology (ALT) and Mount Sopris Co., were used to geophysically log the selected wells. The tools were suspended and driven by an ALT MGX II winch system, powered by a generator in the field. Data were collected and viewed live using the Mount Sopris Instrument Co. programs MSLog and MSHeat. The first tool deployed in each borehole was the fluid temperature and resistivity (2PFA-1000) probe with a temperature resolution of 0.1°C and a fluid resistivity resolution of 0.05 Ohm-m with a sample frequency of 1 s. This tool was run at a rate of

Table 1 Physical characteristics of geophysically logged wells. *Elev. masl* elevation, meters above mean sea level, *L/m* litres per minute, *FPF* foliation parallel fracture, *NA* not applicable. 1 inch=2.54 cm

Well ID	Year drilled	Diameter (inch)	Elev. masl	Yield (L/m)	Thickness (m)	Setting	Aquifer type	Distance to major fault	Rock type	Total depth (m)
Act1	Unknown	6	56	18.9	3	Valley	Unconfined	~2 km	Schist	152
Act2	2005	5.75	50	7.6	0	Valley	Unconfined	~3 km	Schist	181
Act3	2005	5.75	50	7.6	0	Valley	Unconfined	~3 km	Schist	75
Bol3	2006	6	139	3.8	11.6	Valley	Confined	~100 m	Schist	97
Box1	2005	5.75	93	2.8	9	Valley	Confined	~100 m	Schist	97
Gates1	2004	6	90	18.9	3	Valley	Confined	~2.6 km	Schist	182
Gates2	2004	5.75	88	18.9	2	Valley	Confined	~1 km	Schist	178
Gates3	2004	5.75	88	18.9	2	Valley	Unconfined	~1 km	Schist	241.7
Har1	Unknown	<5.75	130	11.4	2	Valley	Unconfined	~1 km	Schist	243
Nor1	Unknown	6	138	Unknown	0	Ridge	Unconfined	~600 m	Schist	171
May2	1999	5.75	61	227.1	10	Valley	Confined	~200 m	Schist	29
Roc1	Unknown	5.75	37	227+	3	Coastal	Confined	~150 m	Amphibolite-gneiss	183
Roc2	Unknown	6	40	227+	3	Coastal	Unconfined	NA	Granite	136
Shr1	2004	5.75	173	56.8	8	Ridge	Unconfined	NA	Granite	168
Sto1	2007	5.5	74	302.8	6	Valley	Unconfined	~800 m	Amphibolite	214
Sut1	Unknown	6	178	3.8	2	Base of hill	Confined	~400 m	Amphibolite-gneiss	92
Top1	2002	5.75	31	3.8	19	Ridge	Unconfined	~20 m	Granite-gneiss	366
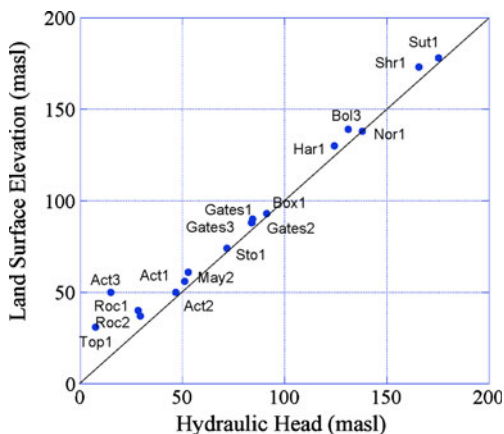
Fig. 2 Hydraulic head measurements at the time of borehole logging plotted against the land surface elevation with sea level as a datum. Most wells fall close or near to the 1 to 1 line. Data suggest a topographically driven flow system

0.3 m/min for all wells. Fluid resistivity and its corresponding inverse property fluid conductivity were measured at each borehole prior to any borehole disturbances, which more or less reflect ambient conditions in equilibrium with the surrounding fluids. Fluid conductivity is a measure of the ability of an aqueous fluid to conduct an electrical current. Variations in the fluid conductivity may result from concentration or the number of ions dissolved in the fluid, mobility of the dissolved ions, the ion oxidation state (or valence), and the temperature of water. Other than an increase in dissolved species in the surrounding fluid, boreholes in fractured rock may trap higher salinity or dense fluids in a dead zone located below active fractures and the bottom of a borehole. Focus in this study was specifically on the overall trend of fluid conductivity with depth and the identification of stepwise changes in fluid conductivity above the bottom of the borehole.

The second tool in the suite was the three-armed caliper probe (2PCA-1000) which measures borehole diameter at a resolution of 0.5 mm. This tool was run at a rate ranging from 0.15 to 0.3 m/min depending on individual well conditions. The next tool in the suite was the optical televiewer, or OTV (ALT OBI), which contains a charge-coupled device (CCD) camera with a three-axis magnetometer/inclinometer that spins in the borehole while taking digital images with a standard resolution of 2 mm. The last tool in the borehole geophysical suite was the acoustic televiewer (ATV–ALT FAC40) capturing high-resolution acoustic imagery at a resolution of 2 mm. Logging speeds for both the OTV and ATV tools were run at a constant rate of 0.1 m/min for all wells. Borehole conditions varied very little between boreholes and the quality of the logs for each well was similar.

The final tool employed in this study suite was the heat pulse flow meter (HFP-2(4)293), which measures the vertical component of fluid flow rate in the borehole at a resolution of 0.2 L/m to determine hydraulically active fractures; flow-meter measurement range is 0.1–3.8 L/min with a resolution of 5%. Measurements are made by lowering the heat pulse flow meter to the bottom of the

borehole. The meter is subsequently raised and measurements of flow rate are taken above and below fractures whose locations are determined from the OTV, ATV and caliper logs. Flow rate is measured by taking the vertical speed and multiplying it by the cross-sectional area of the tool. By taking measurements above and below a specific fracture one can determine whether the fracture is adding or removing fluid to the borehole by examining the change in flow rate compared to the previous measurement.

In a typical hole, over 20 flow-rate measurements were taken. In holes with a significant number of fractures such as Gates1, periodic measurements (such as a measurement every 10 m) were taken during the traverse up the hole, and if no change in flow rate was observed, the meter was moved to the next location. The lack of a change in flow rate from measurement to measurement indicates that the fractures within these windows are not contributing to flow into or out of the borehole.

After traversing the complete hole under ambient conditions, a submersible Grundfos pump and a pressure transducer were lowered into the hole to repeat the flow measurements under pumping conditions. The pumping rate used in this study was approximately 2 L/min. The pressure transducer was used to measure changes in hydraulic head in the borehole and to determine when a steady-head level was reached for the given flow rate. Only under these conditions will the flow rate out of the pump be equal to the volume of water per time entering the borehole. Under pumping conditions, measurements of borehole flow rate should increase as the tool is moved up the hole until the total flow rate in the borehole is equal to the steady-state pumping rate. If two consecutive flow measurements had the same flow rate, observed fractures between the locations of the measurements are considered to not be contributing to flow. This report focuses only on whether or not a fracture contributed to flow into or out of the well and not the magnitude of flow contributed by discrete fractures.

Processing geophysical logs

The program WellCAD (ALT) was used to post-process the borehole geophysical logs. In this program, the fluid temperature and resistivity, gamma, caliper, OTV and ATV dataset files are imported into the program and depth is corrected based on known borehole characteristics such as the depth to casing. Image logs (OTV and ATV) are oriented to magnetic north. All wells visited have deviations less than 1° from vertical.

Once logs are properly aligned and oriented, fractures are identified and measured. Determining which features displayed in the logs are actual fractures is difficult and often a subjective process. In this study a fracture is defined based on the appearance of a visible fracture in the OTV log, or an anomaly in the ATV log (Fig. 3). In either case, the fracture must be visible in both the ATV and OTV logs, or a combination of the caliper and either the OTV or ATV image logs. Once a fracture is identified in an image log, other logs are scanned for evidence of a fracture. Common evidence of a fracture in other logs

includes: a positive (or negative) excursion in the caliper log, a change in lithology seen on the OTV log, or a shift in temperature or fluid resistivity. Each fracture is traced in WellCAD and the depth, orientation, and dip of the fracture is determined. Dipping fractures appear as a sinusoidal line on the unwrapped borehole images; higher amplitudes are associated with steeper dipping fractures and a horizontal line represents a horizontal fracture. Dip direction is read at the peak amplitude from the oriented log and the dip taken from the magnitude of the amplitude. Dip directions are then converted to strike providing strike and dips using the right hand rule convention. Fracture type is then assigned based on a classification scheme of FPF, tectonic joints, and subhorizontal sheeting joints (Manda et al. 2008). FPF fractures are assigned based on whether or not they are parallel to observed foliation in the OTV log. Fractures that are shallower than 25° and are not parallel to foliation are assigned as subhorizontal fractures. The remainders are considered to be tectonic joints.

Hydraulically active (or flowing) fractures are defined here as those fractures previously identified from the image logs that, when tested (using the heat-pulse flow meter) either under ambient (non-pumping) or stressed (pumping) hydrologic conditions, contribute or remove water from the borehole. Contribution of water to the borehole was determined from examination of the heat-pulse flow measurements. Measurements of flow rate below and above fractures are used to make this determination. Over 1,300 measurements of borehole flow rate were performed during this study.

Results

A total of 1,941 fractures were identified and measured in the 17 wells studied, 15 in the Nashoba Terrane and two (Roc1 and Roc2) located in the Avalon Terrane; a total of 2,941 m were logged with an average fracture density of 0.66 fractures per meter (Table 2). The average depth of

the logged wells was 173 m with a range from 366 m for the deepest well and 29 m for the shallowest. Thickness of glacially derived overburden ranged from 0 to 19 m with an average of 4.9 m. The yields reported by drillers ranged from less than 4 L/min to greater than 300 L/min with the majority of wells ranging from 4 to 20 L/min. Wells studied were completed in three bedrock types: amphibolite, schist and granite. Figure 1 depicts the locations of boreholes relative to terrane structure and geology.

Fracture orientations

Three main fracture types are identified in the Nashoba and Avalon terranes: FPF, subhorizontal sheeting joints (dip less then 25°), and tectonic joints. Orientation data were analyzed as follows. Data were first plotted on lower-hemisphere, equal-area stereonets to distinguish sheeting joints from more steeply dipping fractures. Next, azimuths of steeply dipping fractures (dip >60°) were assembled as azimuth frequency histograms and mean trends of peaks determined by fitting Gaussian (normal distribution) curves to smoothed histograms (Wise and McCrory 1982; Wise et al. 1985; Mabee et al. 1994). One standard deviation is equal to the width of the fitted Gaussian curve at half height. Azimuths falling within ±1SD (standard deviation) are assumed to be part of the same population of fractures. Mean trends of peaks outside 1SD are considered to represent a different fracture set. FPFs strike northeast (052°±15°) and dip 70° northwest. The tectonic joints exhibit two main sets. The more prominent set strikes 263°±13° (east west) and dips 72° to the north. The second major set strikes 176°±13° and dips 75° to the west. There are also two minor fracture sets: a north northeast trending set (030°±7° dipping 75° northwest) and a northwest trending set (317° ±7° dipping 68° northeast). Figure 4 illustrates a typical example of the fracture distribution and properties of the boreholes studied. FPF comprise approximately 39% of the total fractures in the terrane. Tectonic joints comprise 51% of the total fractures measured, whereas the subhorizontal sheeting joints comprise the remaining 10%.
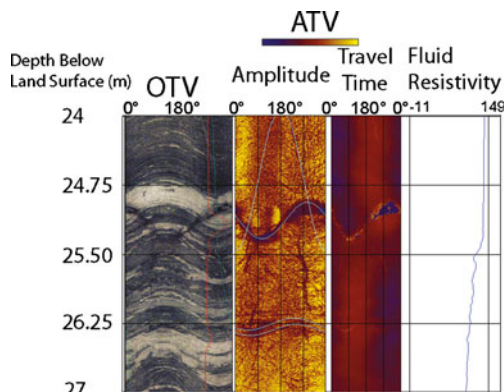
Fig. 3 Example 3-m section of optical televiewer (*OTV*), caliper (*red line*), acoustic televiewer (*ATV*; amplitude and travel time), and fluid resistivity logs. Features that can be indentified in either ATV or OTV, and caliper logs are considered to be fractures

Fracture spacing and depth distribution

One of the main goals of this study is to determine the statistics of fracture occurrence, type, and spacing with depth in the Nashoba and Avalon terrane. A cumulative distribution of fractures with depth below the land surface is presented in Fig. 5a. In general, most of the wells are cased 10 m below the land surface and the region above this area is not available for logging, therefore most wells show fractures beginning at some depth below land surface. A wide range in the total number of fractures intersecting the boreholes is observed with the range extending from 35 to 348 fractures. In the upper parts of most boreholes, the slope of the cumulative fracture versus depth line is linear with variable slope. The slope of this line is equivalent to the borehole fracture spacing (see discussion in the following). Most boreholes show a

Table 2 Fracture statistics of the studied wells. *NP* test not performed

| Well ID	Total depth (m)	Total no. of fractures	No. of FPFs	No. of tectonic fractures	No. of sub-horizontal fractures	Fracture intensity (L/m)	Depth to water (m)	Drawdown (m)	No. of flowing fractures
Act1	152	25	1	17	7	0.16	5.02	NP	2
Act2	181	35	7	20	8	0.19	3.32	0.35	3
Act3	75	13	3	7	3	0.17	35.00	NP	0
Bol3	97	36	21	10	5	0.37	7.84	NP	4
Box1	182	212	86	84	42	1.16	1.88	5	1
Gates1	178	255	63	166	26	1.43	5.69	0.07	5
Gates2	241.7	185	116	49	20	0.77	4.04	0.11	3
Gates3	243	149	38	99	12	0.61	4.21	0.2	4
Har1	171	89	25	56	8	0.52	5.64	0.3	5
Nor1	29	42	14	13	15	1.45	0.00	1.2	2
May2	183	83	0	77	6	0.45	8.16	0.13	5
Roc1	136	133	20	112	1	0.98	7.61	0.14	4
Roc2	168	127	29	96	2	0.76	11.66	0.8	3
Shr1	214	95	68	24	3	0.44	7.36	0.23	4
Sto1	92	62	27	13	22	0.67	2.22	1.19	6
Sut1	232	52	21	23	8	0.22	2.74	0.79	2
Top1	366	348	203	136	9	0.95	23.53	NP	–

steepening of this slope with depth suggesting that fractures are becoming more widely spaced. For example, the Tops1 and Gates2 wells show a strong increase in slope at depths greater than 150 m. A plot of the cumulative number of fractures normalized by the total number of fractures for the individual borehole depicts this trend more clearly for all boreholes (Fig. 5b). Other well sites such as the Act1 and Act2 wells show many fewer fractures and larger fracture spacings with depth (Fig. 5b). In addition, Gates1 and Gates2 are 30 m apart and in the same rock type yet the cumulative fractures are quite different indicating high variability over short spatial lengths. Tops1 is located in the Bloody Bluff Fault Zone, a significant terrane bounding fault. The cumulative number of fractures is high, but not appreciably higher than other logged wells. However, yield from this well is low suggesting limited connectivity between fractures. No trends of increasing fracture intensity with proximity to mapped faults is observed.

A detailed analysis of the fracture spacing for the composite wells was performed on the individual fracture types. Figure 6 depicts the fracture spacing distributions for the individual fracture types in a semi-log plot of frequency versus log fracture spacing. The solid lines reflect fractures detected at all depths whereas dashed lines reflect those fracture types encountered in the upper 100 m of the wells, and dotted lines reflect fractures below 100 m. Fracture spacings appear to follow a log-normal spacing distribution. Comparing fracture spacing distributions in the upper 100 m (dashed lines) to below 100 m (dotted lines) it is clear that the distributions have slightly different median values. FPF and potentially tectonic joints suggest that there are more fracture spacings greater than 10 m below 100 m in all the wells. Sheeting joint distributions indicate slightly higher median fracture spacing values and a tendency to have an equal or greater number of large (>10 m) fracture spacings compared to FPF and tectonic joints.

Table 3 presents a summary of fracture spacing statistics for FPF, tectonic, and sheeting fractures. To investigate the distinct change in characteristics below and above 100-m depth, one needs to calculate a mean and standard deviation of fracture spacings only for the upper 100 m and below 100 m, and a separate calculation for all depths. The mean fracture spacing for all fractures at all depths is 2.7 m, with a standard deviation of 6. FPF and tectonic joints have similar mean spacings but sheeting joints show a larger mean value. In the upper 100 m, these mean values decrease for all fracture types to values 1.8, 1.7, and 5.1 m for FPF, tectonic, and sheeting joints, respectively. For depths greater than 100 m, mean fracture spacing of FPF and tectonic joints increases slightly to 3.3 and 3.3 m respectively (less than 1.5 times), but the spacing of sheeting joints is increased two-fold. A measure of the degree of clustering of fracture sets determined by the parametric fracture spacing statistics, the mean and standard deviation, is the coefficient of variance. The coefficient of variance (C_v) is defined as the ratio of the standard deviation of fracture spacing divided by the mean of the fracture spacing (Gillespie et al. 2001). The C_v expressed the degree of clustering along borehole fracture populations (Gillespie et al. 1993). If fractures are clustered the C_v is greater than 1, while if C_v is less than 1 fractures are anti-clustered or regularly spaced. The C_v is calculated for distinct fracture types for all depths, the upper 100 m of all boreholes, and the lower 100 m of all boreholes. Values of C_v for all of the fractures are greater than 1 (meaning clustered) with varying degrees of clustering. For the upper 100 m the FPF, tectonic, and sheeting joints have C_v values of 1.7, 1.6, and 1.5 respectively, whereas below 100 m those values become 1.7, 1.8, and 2.3. Only the sheeting joints become substantially more clustered.

Despite differences between individual wells in general, a decrease in fracture intensity is observed with depth, as suggested by the fracture spacing distributions. Figure 7 depicts the total number of fractures encountered
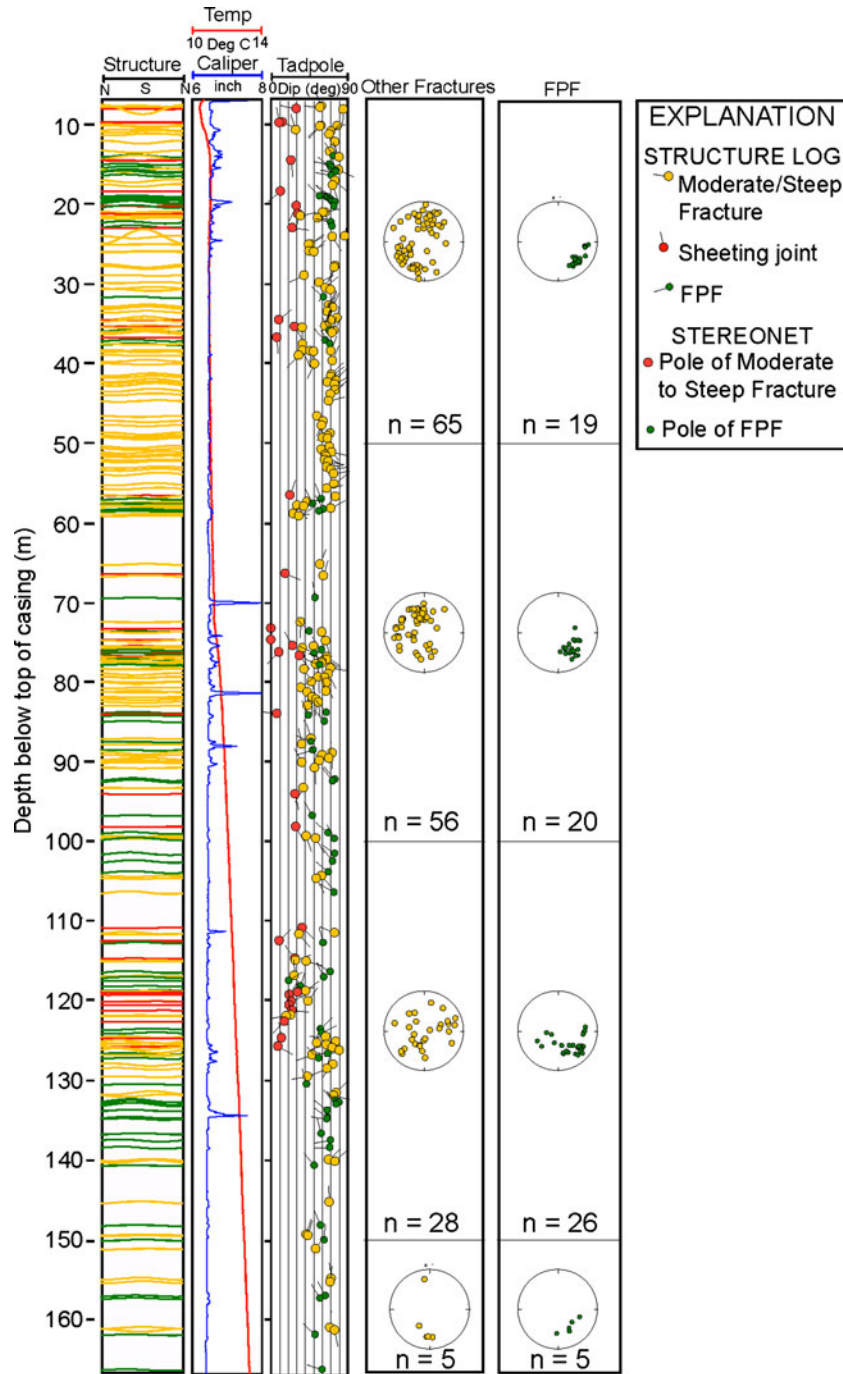
Fig. 4 Gates1 composite log depicting interpreted structure log, depth profiles of caliper and temperature logs, and tadpole and stereo plots (lower hemisphere, equal area projection) of fracture orientations. 1 inch=2.54 cm

within a 15-m interval divided by the total length of boreholes that penetrate a given interval (interval size×no. of wells at that depth) yielding a fracture intensity (L/m). A clear decrease in the total number of all fractures per length of borehole is observed (black solid line), consistent with the cumulative fracture plots for individual wells. To remove the effect of Top1, which, as discussed, sits close to a major terrane-bounding fault and has a large number of fractures, this cumulative fracture intensity is

plotted without the fractures from Top1 (black dashed line). These two lines are roughly identical and show a similar decrease in fracture intensity with depth. Also plotted are the fracture intensities for the distinct fracture types for all wells. FPF and tectonic fractures have the highest intensities and both show a decrease in intensity with depth. The sheeting joints show their largest intensity at shallow depths and drop off with depth but with a minor increase in intensity at 175 m.
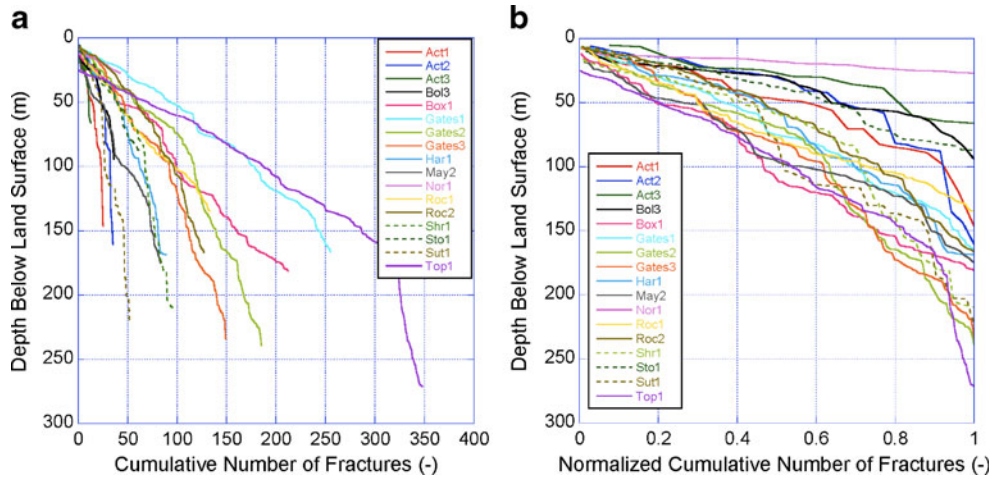
Fig. 5 **a** Cumulative distribution plot of encountered fractures with depth in all boreholes from geophysical logging. **b** Cumulative number of fractures versus depth normalized by the total number of fractures encountered in a given well. A wide number of total fractures are observed in all the boreholes yet most show a steepening slope at deeper intervals suggesting an increase in fracture spacing and a corresponding decrease in total fractures

Hydraulically active fractures

Of the fractures observed in the boreholes, only 2.5% of them are hydraulically active (see section Methods). This is a very small percentage but entirely consistent with the qualitative observations at Mirror Lake and Äspö (e.g., Snow 1968; Shapiro and Hsieh 1991; Shapiro and Hsieh 1994; Mazurek et al. 2003). Every fracture that contributed to flow under ambient conditions also flowed under pumping conditions, but the opposite statement was not necessarily true. More fractures exhibited flow under pumping conditions than under ambient conditions. Three major sets of flowing fractures are observed: northeast trending, north–south trending, and subhorizontal sheeting. Of the flowing fractures, 32% are classified as FPF,
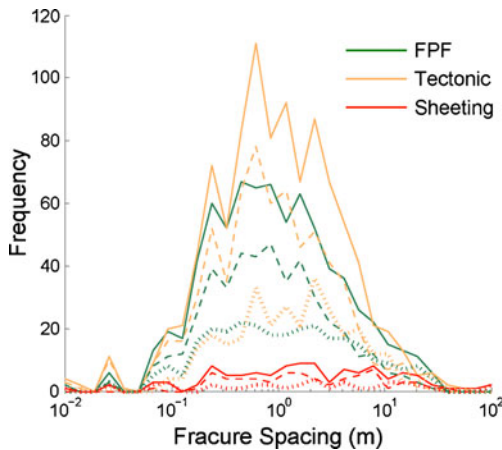
Fig. 6 Fracture spacing histogram for distinct fracture types encountered in all boreholes. *Solid lines* correspond to fractures encountered for all depths, *dashed lines* correspond to those fractures encountered in the upper 100 m of all boreholes, whereas *dotted lines* correspond to fractures below 100 m. Fracture spacing is plotted on a log scale and indicates an approximately log-normal distribution. Distributions are distinct for the upper 100 m compared to those below 100 m

17% subhorizontal, and the remaining 51% tectonic joints. The breakdown of flowing fractures compares reasonably with the overall breakdown of all fractures. However, the subhorizontal sheeting joints have a slightly higher percentage of hydraulically active features. No attempt was made to estimate individual fracture transmissivities but borehole scale transmissivities are discussed in the following.

The depth distribution of hydraulically active fractures in all of the boreholes exhibits a decreasing trend. No hydraulically active features are found beneath a depth of 165 m (Fig. 8a). Most hydraulically active fractures (greater than 70%) are in the upper 100 m, with a large percentage of those even shallower. FPF and tectonic fractures show approximately constant fracture intensity with depth until they ultimately disappear below 165 m. Hydraulically active sheeting joints disappear before that depth, explaining the elevated number of hydraulically active fractures at shallow depths. Even though only 2.5% of the total fractures are hydraulically active, the percentage of flowing fractures also changes with depth (Fig. 8b). Hydraulically active fractures range from 6% of the fractures within 15 m of the ground surface and decreases to the zero below 165 m. These percentages indicate not only a decrease in the number of hydraulically active fractures with depth but also reflect a decrease in the percentage of the total fractures, which contribute to fluid movement in and out of the borehole.

The spatial orientation of hydraulically active fractures with depth is presented in Fig. 9. The equal area stereonets plot the poles to planes of fracture orientations, projected in the lower hemisphere grouped into 30-m-depth intervals. Two observations are noteworthy. First, the number of hydraulically active fractures is high in the upper 30 m with several orientation sets participating in flow including northwest, north–south, east–west and northeast trending sets. At 60 and 90-m depths, the number of hydraulically active fractures is reduced but the fractures

Table 3 Fracture spacing distributions for distinct fracture types. *SD* standard deviation

	All fractures	FPFs	Tectonic fractures	Sheeting fractures
All depths				
Mean (m)	2.7	2.4	2.3	7.7
Median (m)	0.9	0.9	1.0	1.9
SD (m)	6.0	4.4	4.3	16.7
Coefficient of variance	2.2	1.8	1.9	2.2
<100-m depth				
Mean (m)	2.0	1.8	1.7	5.1
Median (m)	0.8	0.8	0.8	1.7
SD (m)	3.5	3.2	2.7	7.8
Coefficient of variance	1.8	1.7	1.6	1.5
>100-m depth				
Mean (m)	3.8	3.3	3.3	10.1
Median (m)	1.3	1.1	1.4	2.1
SD (m)	8.2	5.5	6.1	23.1
Coefficient of variance	2.2	1.7	1.8	2.3

that remain active are associated with the north–south, east–west and northwest trends. The influence of FPF (northeast trending fractures) is reduced. Below 90-m depth, there are too few flowing fractures to draw meaningful conclusions. Second, the hydraulically active sheeting joints (those with dips <25°) disappear after 100 m. Fractures with dips greater than 40° appear to be supporting flow at deeper depths.

Borehole fluid properties

In addition to the active and physical property measurements discussed previously, properties of the fluids filling the boreholes can also give an indication as to the nature of fluid saturating the fractures outside of the borehole. Figure 10 depicts seven logs of fluid electrical conductivity from boreholes involved in this study that are
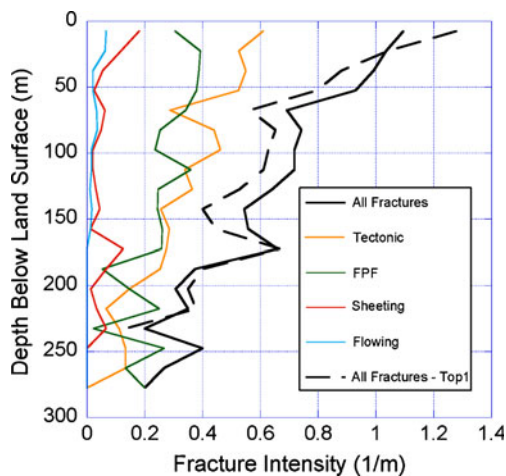

Fig. 7 Composite depth distribution of all fractures encountered in the 17 boreholes in this study. Total number of fractures encountered within a 15-m interval are summed and divided by the total length of borehole in that interval (interval size×no. of wells at that depth) to yield fracture intensity (L/m). All fractures are plotted with (*black solid line*) and without (*black dashed line*) the influence of the Top1 well. Additionally, distinct fractures types and flowing fractures are depicted. All fracture distributions show a decrease in intensity with depth

representative of conditions encountered in all of the boreholes. The corrected conductivity logs show a similar pattern of general increase in conductivity with depth punctuated by sharp (and a few gradual) changes in conductivity. Step changes in conductivity with straight linear portions immediately below them suggest the discrete mixing of either higher conductivity fluid moving down the borehole or dilution of the borehole with lower conductivity fluid moving upward. For example, the Gates1 well shows a complex pattern of conductivity increase with depth. Below the water table, at least three sharp discrete changes in conductivity occur that are correlated to flowing fractures in this hole. Below active flowing fractures pooling or concentration of a fluid with slightly higher conductivity is observed in a number of profiles. The gradual sloping change in conductivity from 80 to 130 m is not as easy to explain but appears to have a few discrete inflections in the slope of the conductivity profile. In general, all of the discrete step wise changes in conductivity occur above 150-m depth and most are shallower than 100 m supporting the previous observations of restricted deeper circulation of fluids. There is a tendency for a fluid to increase its total dissolved solids concentration (a quantity related to fluid conductivity) as the amount of contact time with rock increases. The increase in fluid conductivity with depth suggests that these fluids have longer residence times than the shallower borehole fluid.

Borehole temperature profiles

Temperature profiles and temperature variations in boreholes are the direct result of both the conductive and advective transport of heat in the sub-surface (Anderson 2005). The use of sub-surface temperature measurements to estimate advective velocity of groundwater is becoming more commonplace as inexpensive equipment and technology are available for a broad range of deployments. Additionally, qualitative statements and analyses of these profiles yield important information concerning the activity of subsurface flow regimes. Temperature profiles were collected at each borehole (Fig. 11) during logging. The
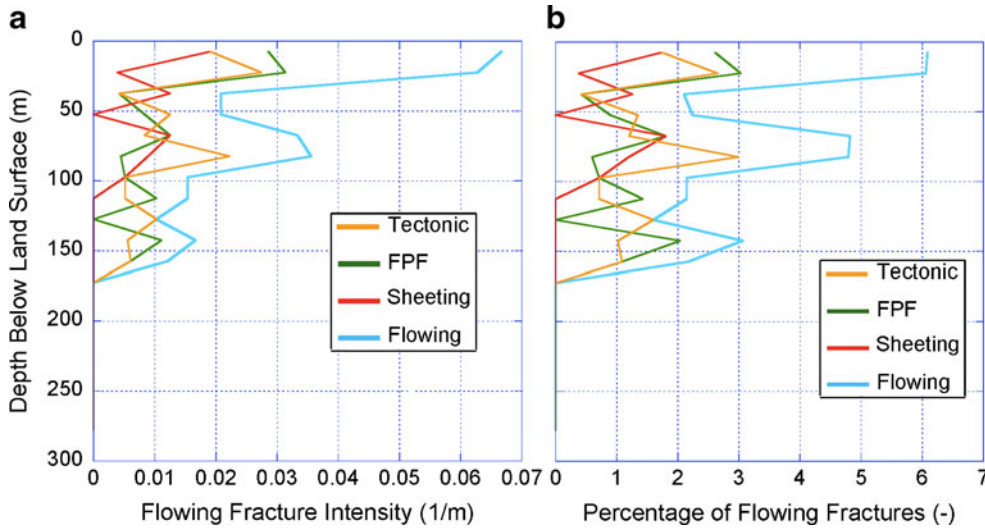
Fig. 8 **a** Composite fracture intensity (15 m intervals) line plots of all hydraulically active fractures (*blue lines*), i.e., those which have measurable flow into the borehole under stressed (pumping) conditions as determined by over 1,300 individual heat pulse flow meter measurements. No fractures below 165 m were observed to be hydraulically active during testing. Hydraulically active FPF, tectonic, and sheeting joints are also depicted. **b** Composite (15 m bins) line plots of all hydraulically active fractures (*blue lines*) expressed as a percentage of total fractures encountered at that depth

sensitivity of these temperature measurements is +/– 0.1° C with a vertical sample resolution of 0.1 m. Almost every profile shows an increase in temperature with depth. In the upper 100 m, the temperature profile is influenced heavily by surface-driven heating and cooling as well as shallow circulation of meteoric fluids. The profiles suggest a strong relationship between seasonal temperature variations and subsurface variations in temperature in the upper 30 m.

Below 30 m, deviations in the profiles from a conductive signature suggest movement of heat through advection of fluids to roughly 100 m. Deviations from a linear heat conduction profile suggest the movement of fluid within the borehole through permeable and hydraulically active fractures. These are represented as step changes in temperature, deviations in slope causing near constant temperature profiles, and small deflections in temperature from the conductive profile. All correlate with the previous independently determined hydraulically active fractures. Below a depth of about 100 m, almost all of the profiles show strong conductive-like linear increase of temperature with depth and a slope ranging from 13 to 23°C per km.

Borehole hydrologic properties

Specific capacity, transmissivity, and hydraulic conductivity of the boreholes were calculated. Hydraulic head was monitored in each borehole using a pressure transducer equipped with a data-logger during pumping. Flow (volume of water discharging from the pump) was measured at regular intervals. Steady-state drawdown was determined as the long-time asymptote of the hydraulic head versus time data. Drawdown data from pumping tests at each well were used to calculate the

specific capacity (SC) of each well using the Cooper-Jacob Solution

$$\text{SC} = \frac{Q}{S_w} \tag{1}$$

Here Q is constant discharge (m^3/s) and S_w is drawdown (m). The transmissivity, T (m^2/s), of each well can be calculated from SC using

$$\text{SC} = \frac{T}{0.183 \log\left(\frac{2.25Tt}{r_w^2 S}\right)} \tag{2}$$

where t is time (s), r_w is the pumped well radius (m), and S is the dimensionless storativity. Batu (1999) developed simplified equations for T using SC for a confined aquifer
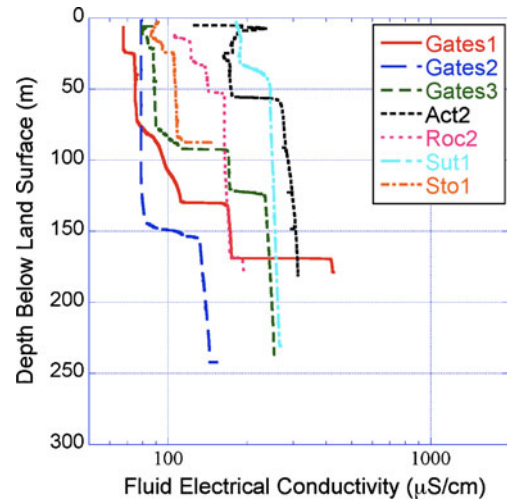
$$\text{T} = 1.385(\text{SC}) \tag{3}$$

From these equations, a borehole hydraulic conductivity (K) can be calculated using $K = T/b$ where b is the length of saturated borehole below the casing. Based on the above assumptions, the average T for the Nashoba wells is 7.4E1 m^2/day, and the average K is 3.4E-01 m/day or 4.0E-06 m/s. The results are qualitatively consistent with yield data reported by well drillers. The wells with the highest hydraulic conductivity are at the Rockport site (Roc1 and Roc2) and this finding is consistent with the results of multi-day aquifer stress tests conducted on these wells for public water-supply development. Hydraulic conductivity measurements from single-well pumping tests tend not to be robust measures of hydraulic conductivity of the adjoining rock mass. Nevertheless, they can be used in this study for comparison purposes.
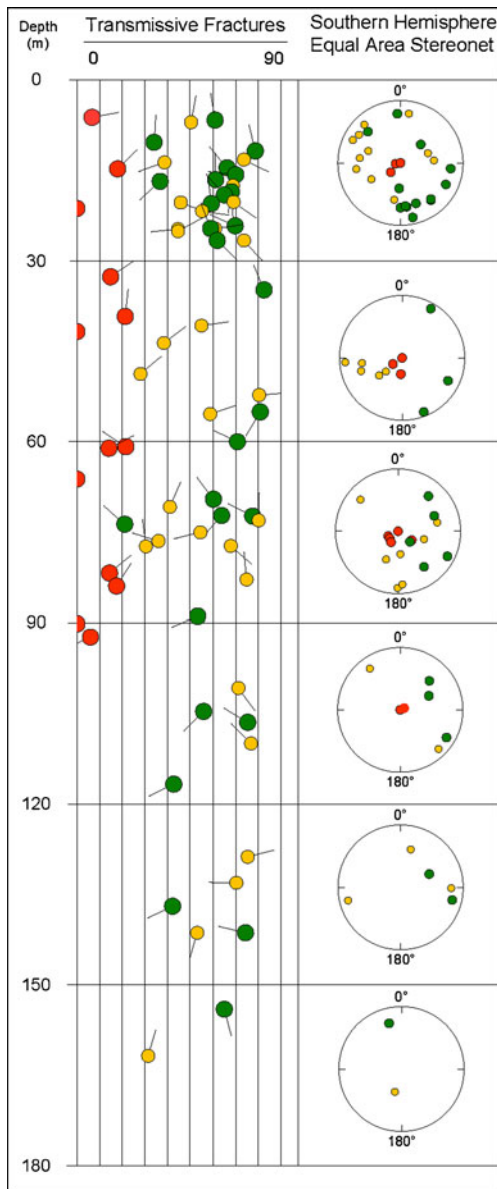
Fig. 9 Tadpole plot of the depth distribution of hydraulically active fractures together with a 30-m-binned equal area lower hemisphere stereonet of fracture orientation. *Dot* indicates the dip, *tail* indicates dip direction. Dip and dip direction converted to strike and dip in stereonet using right-hand rule convention. Shallow dipping sub-horizontal sheeting joints appear to be less common at depths greater than 100 m

Fig. 10 Fluid electrical conductivity profiles for select wells involved in this study. Fluid conductivity in the wells generally increases with depth within the borehole. Step changes in these profiles reflect fluid composition changes of the fluid entering through discrete fractures or zones of fractures

Discussion

The data presented here demonstrate strong and significant trends with increasing depth into the subsurface of these crystalline rocks. Figures 7 and 8 suggest that the frequency of hydraulically active fractures decreases at a rate proportional to the presence of (total) fractures to a depth of 170 m. This is potentially the result of the unresolved relationship between depth, permeability and in situ stress in shallow environments. The positive correlation between the hydraulically active fractures and total fractures observed suggests that the decrease in the number of fractures is a main control on whether a fracture is hydraulically active. This is ultimately an issue
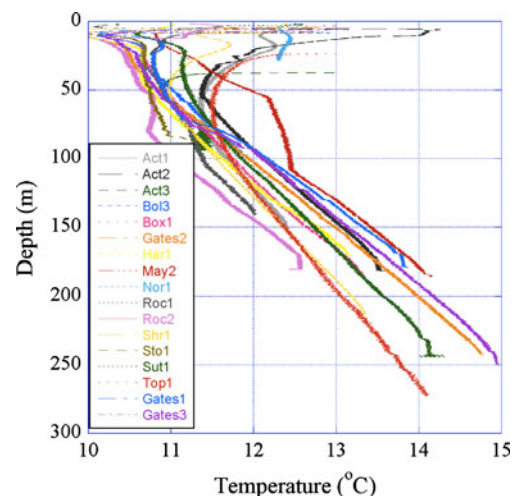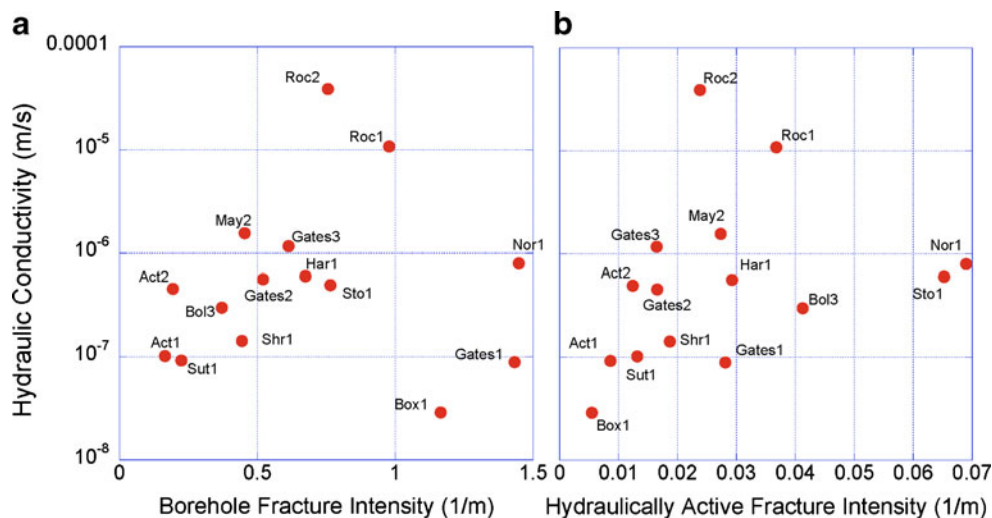
The composite hydraulic conductivity of fractured rock intersecting a borehole is related to the connectivity, aperture, and number of fractures intersecting the borehole. The next step is to examine the relationship between the inferred borehole average hydraulic conductivity and two measures of fractures in the borehole: borehole fracture intensity (Fig. 12a), and hydraulically active fracture intensity (Fig. 12b). A plot of hydraulic conductivity versus the hydraulically active fractures, normalized by borehole length, reduces scatter (compare Fig. 12a–b), but a few outliers remain (namely Nor1 and Sto1). These are two of the shallower boreholes involved in the study, 29 and 92 m deep, respectively.

Fig. 11 Temperature profiles of open-hole boreholes in crystalline rocks collected in the summer of 2007 in the Nashoba and Avalon terranes. All boreholes had been drilled in previous years and are considered to be in thermal equilibrium with the surrounding rock. Profiles suggest advective disturbance of a thermally conductive profile only above 130 m

Fig. 12 Bulk hydraulic properties of boreholes visited in the study area. **a** Estimated hydraulic conductivity of boreholes versus number of fractures observed, divided by length of borehole, to give borehole fracture intensity. **b** Estimated hydraulic conductivity of boreholes versus number of hydraulically active fractures observed, divided by length of borehole, to give hydraulically active fracture intensity. Act3 did not have any hydraulically active fractures detected within the sensitivity of the instruments used and no drawdown data are available for Top1

of fracture connectivity. Despite these observations, the physics of this process remains an unresolved issue (Snow 1968; Legrand 1954; Legrand 1967; Davis and Turk 1964). Laboratory studies have shown that fracture apertures decrease at greater rates under small stresses (>5 MPa; Bandis et al. 1983; Brown and Scholz 1986; Hillis 1987), and stiffen at higher stress magnitudes. Therefore, fracture permeability should be most sensitive at shallower depths within the crust. The lack of few hydraulically active subhorizontal fractures below 100 m depth is evidence that subhorizontal sheeting joints play an important role in the connectivity and bulk permeability of fracture networks in igneous and metamorphic rocks. The combined impact of fracture closure (fractures present but closed due to mechanical loading) and decreasing fracture presence (overall decrease in the number of fractures in the rock) cannot be directly investigated with this data, but both are likely to be occurring.

The fracture intensity for all (total) fractures decreases with increasing depth below the land surface. Individual fracture types (FPF, tectonic, and sheeting) similarly depict decreasing intensity with depth, with and without the influence of Top1, a well that is located near a mapped terrane bounding fault. A number of wells in this study are located within a few hundred meters of mapped faults. Evaluation of fracture intensity or flowing fracture intensity with distance from mapped fault does yield statistically significant trends. The number of flowing fractures in these wells or the drillers' reported yields do not suggest any meaningful relationships. The fact that these faults are often heavily deformed and are intensely foliated shear zones suggests that they do not generally increase the fracture intensity and resulting connectivity of fracture networks. Some types of faults have been shown to play an important role in either impeding groundwater flow or driving groundwater flow into deeper flow systems (Seaton and Burbey 2005; Stober and Bucher 2004) and,

thus, will impact or modify this trend. Future work is needed on piecing together the importance of these regional-scale ductile structural elements on permeability structure and flow systems with depth.

Distributions of fracture spacing approximately follow a log-normal distribution for all fracture types. Spacings of tectonic and FPF fractures have similar statistical distributions that are distinctly different from those of sheeting joints. Sheeting joints show larger spacing and are more clustered. The depth dependence of fracture spacing is exhibited in all fracture types as depths less than 100 m show closer spacing compared to fractures below 100 m. Fracture spacing plays an important role in connectivity of fracture networks; thus, the data presented here suggest that the combined decrease in both the numbers of fractures and the total number of hydraulically active fractures will ultimately restrict meteoric topographically driven flow systems to depths of 100 – 150 m. The concept of a broad interconnected water table and aquifer (as typical of more traditional porous media) is not likely to apply in aquifers characterized by these conditions. Previous work has suggested that groundwater is primarily found in saturated fracture clusters and groundwater is transported between them by less transmissive connecting fractures. These connecting fractures are likely to be of variable orientation; however, results of this study suggest that subhorizontal sheeting joints can play an important role in the flow system. It is possible, then, that these subhorizontal joints connect these "saturated clusters".

Conclusions

A detailed regional borehole study was undertaken to evaluate the depth evolution of physical and hydraulic properties of fracture networks in fractured crystalline and metamorphic rock. Seventeen fractured-rock wells (over

3 km of fractured rock) in three distinct lithologies were logged using borehole geophysical tools to detect 1,941 individual fractures in both hydrologically unproductive and productive wells. This study avoids the direct use of driller data (such as yield, encountered fracture statistics, and water-bearing fracture statistics) but relies on high-quality geophysically derived borehole data to answer important questions regarding the depth-dependent physical and hydraulic properties of fractures in the subsurface.

The main conclusions are summarized as follows:

- The observed fracture intensity shows a strong decrease with depth below 165 m.
- Correspondingly, the spacing of all fracture sets increases with depth and in general fractures become more clustered.
- Approximately 2.7% of all fractures were determined to be hydraulically active. The intensity of flowing fractures also decreases with depth.
- Few sub-horizontal features, as opposed to FPF and tectonic fractures, are hydraulically active below 100 m.
- Data on borehole fluid electrical conductivity and temperature both independently support evidence of relatively rapid shallow (<150 m) circulation of meteoric fluids.
- Borehole hydraulic conductivity estimates are positively correlated with the percentage of hydraulically active fractures.
- The decrease in fracture presence at depth appears to influence fracture connectivity and resulting network permeability, but has less influence on hydromechanical coupling (fracture closure).

The cause of this decrease in permeability and, hence, productivity appears to result from a decrease in the density of fracturing with depth giving rise to lower connectivity of the fracture networks. Most of the sites studied here are adjacent or close to regional ductile shear zones so the influence of fracture zones or faults on the permeability structure as a function of depth is not clear. It is uncertain how these relic structures will modify and possibly extend the depth-related results shown here and is the focus of current and future work.

References

Anderson M (2005) Heat as a ground water tracer. Ground Water 43 (6):951–968

Bandis S, Lumsden A, Barton N (1983) Fundamentals of rock joint deformation. Int J Rock Mech Min Sci Geomech Abstr 20 (6):249–268

Barton C (1996) Characterizing bed rock fractures in outcrop for ground-water hydrology studies: an example from Mirror Lake, Grafton County, New Hampshire. In: Morganwalp D, Aronson D (eds) U.S. Geological Survey Toxic Substances Hydrology Program-Proceedings of the technical meeting, Colorado Springs, Colo. US Geol Surv Water Resour Invest Rep 94-4015

Batu V (1999) Aquifer hydraulics: a comprehensive guide to hydrogeologic data analysis. Wiley, New York

Bell K, Alvord D (1976) Pre-Silurian stratigraphy of northeastern Massachusetts, Memoir 148, Geological Society of America, Boulder, CO

Brown S, Scholz C (1986) Closure of rock joints. J Geophys Res Solid Earth 91(B5):4949–4948

Caine J, Tomusiak S (2003) Brittle structures and their role in controlling porosity and permeability in a complex Precambrian crystalline-rock aquifer system in the Colorado Rocky Mountain Front Range. Geol Soc Am Bull 115(11):1410–1424

Caine J, Evans J, Forster C (1996) Fault zone architecture and permeability structure. Geology 24:1025–1028

Castle R, Dixon J, Grew E, Griscom A, Zeitz I (1976) Structural dislocations in Eastern Massachusetts, US Geol Surv Bull 1410

Davis S, Turk L (1964) Optimum depth of wells in crystalline rock. Ground Water 2:6–11

Evans KF, Moriya H, Niitsuma H, Jones RH, Phillips WS, Genter A, Sausse J, Jung R, Baria R (2005) Microseismicity and permeability enhancement of hydrogeologic structures during massive fluid injections into granite at 3km depth at the Soultz HDR site. Geophys J Int 160:388–412

Gillespie PA, Howard C, Walsh LL, Watterson L (1993) Measurement and characterisation of spatial distributions of fractures. Tectonophysics 226:113–141

Gillespie PA, Walsh JJ, Watterson J, Bonson CG, Manzocchi T (2001) Scaling relationships of joint and vein arrays from The Burren, Co. Clare, Ireland. J Struct Geol 23:183–201

Goldsmith R (1991) Stratigraphy of the Nashoba zone, Eastern Massachusetts: an enigmatic terrane. US Geol Surv Prof Pap 1366-E-J

Hatch N (ed) (1991) The bedrock map of Massachusetts, US Geol Surv Prof Pap 1366A-J

Hillis R (1987) The influence of fracture stiffness and the in situ stress field on the closure of natural fractures. Petrol Geosc 4 (1):57–65

Hsieh P (1996) An overview of field investigations of fluid flow in fractured crystalline rocks on the scale of hundreds of meters. In: Stevens P, Nicholson T (eds) Joint U.S. Geological Survey, Nuclear Regulatory Commission Workshop on Research Related to Low-Level Radioactive Waste Disposal, May 4–6, 1993. US Geol Surv Sci Invest Rep 95-4015

Hsieh P, Shapiro A (1996) Hydraulic characteristics of fractured bedrock under lying the FSE well field at the Mirror Lake site, Grafton County, New Hampshire. In: Morganwalp D, Aronson D (eds) U.S. Geological Survey Toxic Substances Hydrology Program: proceedings of the technical meeting, Colorado Springs, Colo. US Geol Surv Sci Invest Rep 94-4015, pp 127–130

Johnson C, Dunstan A (1998) Lithology and fracture characterization from drilling investigations in the Mirror Lake area from 1979 through 1995 in Grafton County New Hampshire. US Geol Surv Water Resour Invest Rep 98-4183

Johnson C, Williams J (2003) Hydraulic logging methods: a summary and field demonstration in Conyers, Rockdale County, Georgia. In: Williams L (ed) Methods used to assess the occurrence and availability of ground water in fractured-crystalline bedrock: an excursion into areas of Lithonia Gneiss in eastern metropolitan Atlanta, Georgia, vol 23. Georgia Geologic Survey, Atlanta, GA, pp 40-47

Legrand H (1954) Geology and ground water in the Statesville area, North Carolina. Bulletin, North Carolina Division of Mineral Resources, Raleigh, NC

Legrand H (1967) Ground water of the Piedmont and Blue Ridge provinces in the southeastern states. US Geol Surv Circ 528

Lyford FP, Carlson CS, Hansen BP (2003) Delineation of water sources for three public-supply wells in three fractured-bedrock aquifer systems in Massachusetts. US Geol Surv Water Resour Invest Rep 02-4290, 114 pp

Mabee S, Salamoff S (2006) Fracture characterization map of the Marlborough quadrangle, Massachusetts, Geologic Map GM06-02, Massachusetts Geological Survey, Cambridge, MA

Mabee SB, Hardcastle KC, Wise DU (1994) A method of collecting and analyzing lineaments for regional-scale fractured-bedrock aquifer studies. Ground Water 32(6):884–894

Mackie D (2002) An integrated structural and hydrogeologic investigation of the fracture system in the upper Cretaceous Nanaimo group, southern Gulf Islands. MSc Thesis, Simon Fraser University, Canada

Manda A, Mabee S, Wise D (2008) Influence of rock fabric on fracture attribute distribution and implications for groundwater flow in the Nashoba terrane, eastern Massachusetts. J Struct Geol 30:464–477

Maréchal JC, Dewandel B, Subrahmanyam K (2004) Use of hydraulic tests at different scales to characterize fracture network properties in the weathered-fractured layer of a hard rock aquifer. Water Resour Res 40, W11508. doi:10.1029/2004WR003137

Mazurek M (2000) Geological and hydraulic properties of water-conducting features in crystalline rocks. In: Stober I, Bucher K (eds) Hydrogeology of crystalline rocks. Kluwer, Dordrecht, The Netherlands, pp 3–26

Mazurek M, Jakob A, Bossart P (2003) Solute transport in crystalline rocks at Äspö: geological basis and model calibration. J Contam Hydrol 61:157–174

Meinzer O (1923) The occurrence of ground water in the United States. US Geol Surv Water Suppl Pap 489

National Research Council (1996) Rock fractures and flow: contemporary understanding and applications. National Academy Press, Washington, DC

Paillet F (1985) Geophysical well log data for study of water flow in fractures near Mirror Lake. US Geol Surv Open-File Rep 85-340

Paillet F, Kapucu K (1989) Fracture characterization and fracture-permeability estimates from geophysical logs in the Mirror Lake watershed, New Hampshire. US Geol Surv Water Resour Invest Rep 89-4058

Park Y-J, Cornaton F, Normani S, Sykes J, Sudicky E (2008) Use of groundwater lifetime expectancy for the performance assessment of a deep geologic radioactive repository: 2. application to a Canadian shield environment. Water Resour Res 44(4), W04407. doi:10.1029/2007WR006, 212 pp

Robinson P, Goldsmith R (1991) Stratigraphy of the Merrimack belt, central Massachusetts. In: Hatch N (ed) The bedrock geology of Massachusetts, part II. US Geol Surv Prof Pap 1366E-J, pp G1–G37

Robinson P, Ratcliffe NM, Hepburn JC (1993) A tectonic-stratigraphic transect across the New England Caledonides of Massachusetts. In: Cheney JT, Hepburn J (eds) Guidebook for field trips in the northeastern United States, Geological Society of America Annual Meeting in Boston. University of Massachusetts, Amherst, MA, Contribution No. 67-1, pp C1–C47

Ruqvist J, Stephansson O (2003) The role of hydromechanical coupling in fractured rock engineering. Hydrogeol J 11(1):7–40

Seaton W, Burbey T (2005) Influence of ancient thrust faults on the hydrogeology of the Blue Ridge province. Ground Water 43 (3):301–313

Shapiro A, Hsieh P (1991) Research in fractured-rock hydrogeology: characterizing fluid movement and chemical transport in fractured rock at the mirror lake drainage basin, New Hampshire. In: U.S. Geol. Survey Toxic Substances Hydrology Program: Proc. of the technical meeting, Monterey, California, March 11–15, 1991. US Geol Surv Water Resour Invest Rep 91-4034

Shapiro A, Hsieh P (1994) Hydraulic characteristics of fractured bedrock underlying the FSE well Field at the mirror lake site, Grafton county, New Hampshire. In: U.S. Geological Survey Toxic Substance Hydrology Program: proceedings of the technical meeting, Colorado Springs, Colorado, September 20–24, 1993. US Geol Surv Water Resour Invest Rep 94-4015

Shapiro A, Hsieh P (1998) How good are estimates of transmissivity from slug tests in fractured rock. Ground Water 36 (1):37–48

Shapiro A, Hsieh P, Burton W, Walsh G (2007) Integrated multi-scale characterization of ground-water flow and chemical transport in fractured crystalline rock at the Mirror Lake site, New Hampshire. In: Hyndman F, Day-Lewis DW, Singha K (eds) Subsurface hydrology: data integration for properties and processes. Geophysical Monograph Series 171, American Geophysical Union, Washington, DC, pp 201–225

Snow D (1968) Rock fracture spacings, openings, and porosities. J Soil Mech Found Div 94(SM 1):73–91

Stober I, Bucher K (2004) Fluid sinks within the earth's crust. Geofluids 4:143–151

Surrette M, Allen D (2008) Quantifying heterogeneity in fractured sedimentary rock using a hydrostructural domain approach. Geol Soc Am Bull 120(1/2):225–235

Surrette M, Allen D, Journeay M (2007) Regional evaluation of hydraulic properties in variably fractured rock using a hydrostructural domain approach. Hydrogeol J 16(1)11–30. doi:10.1007/s10,040-007-0206-9

Tiedeman C, Hsieh P (2001) Assessing an open-well aquifer test in fractured crystalline rock. Ground Water 39(1):68–78

Wise D (2005) Rift and grain in basement: thermally triggered snapshots of stress fields during erosional unroofing of the Rocky Mountains of Montana and Wyoming. Rocky Mt Geol 40(2):193–209

Wise DU, McCrory TA (1982) A new method of fracture analysis: azimuth versus traverse distance plots. Geol Soc Am Bull 93:889–897

Wise DU, Funiciello R, Parotto M, Salvini F (1985) Topographic lineament swarms: clues to their origin from domain analysis of Italy. Geol Soc Am Bull 96:952–967